Global Biogeochemical Cycles

RESEARCH ARTICLE
10.1029/2018GB005983

Modeling the Impact of Zooplankton Diel Vertical Migration on the Carbon Export Flux of the Biological Pump

Kevin M. Archibald[1,2], **David A. Siegel**[3], **and Scott C. Doney**[4]

[1]Department of Biology, Woods Hole Oceanographic Institution, Woods Hole, MA, USA, [2]Department of Earth, Atmospheric, and Planetary Sciences, Massachusetts Institute of Technology, Cambridge, MA, USA, [3]Earth Research Institute and Department of Geography, University of California, Santa Barbara, CA, USA, [4]Department of Environmental Sciences, University of Virginia, Charlottesville, VA, USA

Key Points:
- A novel satellite-driven model of ocean carbon export was developed, including the role of diel vertical migration
- Diel vertical migration is a significant contributor to carbon export out of the euphotic zone, especially in the subtropics
- The export flux mediated by diel vertical migration significantly impacts mesopelagic biogeochemistry

Correspondence to:
K. M. Archibald,
karchibald@whoi.edu

Citation:
Archibald, K., Siegel, D. A., & Doney, S. C. (2019). Modeling the impact of zooplankton diel vertical migration on the carbon export flux of the biological pump. *Global Biogeochemical Cycles*, *33*, 181–199. https://doi.org/10.1029/2018GB005983

Received 22 MAY 2018
Accepted 17 JAN 2019
Accepted article online 19 JAN 2019
Published online 13 FEB 2019

Abstract One pathway of the biological pump that remains largely unquantified in many export models is the active transport of carbon from the surface ocean to the mesopelagic by zooplankton diel vertical migration (DVM). Here, we develop a simple representation of zooplankton DVM and implement it in a global export model as a thought experiment to illustrate the effects of DVM on carbon export and mesopelagic biogeochemistry. The model is driven by diagnostic satellite measurements of net primary production, algal biomass, and phytoplankton size structure. Due to constraints on available satellite data, the results are restricted to the latitude range from 60°N to 60°S. The modeled global export flux from the base of the euphotic zone was 6.5 PgC/year, which represents a 14% increase over the export flux in model runs without DVM. The mean (± standard deviation, SD) proportional contribution of the DVM-mediated export flux to total carbon export, averaged over the global domain and the climatological seasonal cycle, was 0.16 ± 0.04 and the proportional contribution of DVM activity to total respiration within the twilight zone was 0.16 ± 0.06. Adding DVM activity to the model also resulted in a deep local maximum in the oxygen utilization profile. The model results were most sensitive to the assumptions for the fraction of individuals participating in DVM, the fraction of fecal pellets produced in the euphotic zone, and the fraction of grazed carbon that is metabolized.

1. Introduction

Marine food webs help mediate the transfer of atmospheric carbon dioxide downward into the water column via a suite of ecological mechanisms collectively referred to as the biological pump (Falkowski et al., 1998). Photosynthesis by marine phytoplankton fixes carbon dioxide in the ocean's surface into organic carbon, which is passed through the food web. A portion of this carbon sinks out of the euphotic zone in the form of algal cell aggregates and zooplankton fecal pellets, or may be actively transported to depth by zooplankton vertical migrations (Steinberg et al., 2000). The integrated effect of these mechanisms is a downward flux of carbon from the surface ocean deeper into the water column, where carbon may be sequestered in the deep ocean on time scales that are significant for ecological and climate processes (Falkowski et al., 1998).

Quantifying the carbon export flux of the biological pump and understanding how it may change in response to variable climate or biogeochemical conditions is critical to gaining a complete and predictive understanding of the global carbon cycle (Siegel et al., 2014). Since comprehensive global studies of the biological pump are financially and logistically challenging, the development of mechanistic models is an important supplement to field studies. A key step in the development of these models is exploring the impact of different pathways of carbon export (Siegel et al., 2016). In addition to particles that sink out of the euphotic zone, carbon can also be actively transported by the diel vertical migrations (DVMs) of zooplankton (Siegel et al., 2016; Steinberg & Landry, 2017).

Many species of zooplankton participate in DVMs, spending the dark hours of the night in surface waters to graze on phytoplankton and smaller zooplankton, then migrating to depth during the day and simultaneously transporting grazed carbon with them (Longhurst et al., 1990; Steinberg & Landry, 2017). This behavior may be a response intended to reduce predation by visual predators in the well-lit surface waters during the daylight hours (Hays, 2003; Lampert, 1989). A portion of the carbon that is grazed at the surface

during the night is metabolized or deposited as fecal pellets in the twilight zone during the day, thereby contributing to the export of carbon to below the euphotic zone (Steinberg et al., 2002).

A number of modeling studies have quantified the regional contribution of zooplankton DVM to the carbon export flux in a variety of environments and consistently found a significant effect of DVM on the biological pump (Bianchi, Stock, et al., 2013; Putzeys & Hernandez-Leon, 2005; Wallace et al., 2013). Work by Bianchi, Stock, et al. (2013) concluded that carbon transported via DVM accounts for 10–30% of the total particulate flux and as much as 50% of the metabolic carbon dioxide produced in the twilight zone. These results underscore the importance of spatially decoupling grazing from zooplankton respiration and the production of fecal pellets and demonstrates the strong influence that DVM can have on mesopelagic biogeochemistry (Bianchi, Galbraith, et al., 2013). Still, the DVM transport pathway remains an uncommon feature in biogeochemical models of carbon export and the global contribution of DVM-mediated export is largely unquantified.

This study extends the work of Siegel et al. (2014) by quantifying the contribution of DVM activity to the total export flux of the biological pump and exploring the effect of DVM on mesopelagic biogeochemistry. We apply the model to a global domain to compare how variable forcing conditions change how DVM contributes to the biological pump. Because the underlying food web model is driven diagnostically with satellite ocean color data, the expanded euphotic zone-mesopelagic model provides capability to estimate time-evolving DVM globally over seasonal cycles, as well as estimate interannual variability. The model is introductory in nature and we make a number of simplifying assumptions concerning zooplankton population dynamics and DVM behavior in order to explore the broad-scale implications of DVM-mediated export and the effects on twilight zone biogeochemistry. Our hope is that this model will contribute to a mechanistic understanding of the role of zooplankton populations in the biological pump.

2. Methods

2.1. Constructing the Model

The model is constructed using two components—the existing euphotic zone module (Siegel et al., 2014) and a new twilight zone (mesopelagic) module. The euphotic zone component uses a food web model forced by satellite observations of net primary production (NPP) and the time rate of change in phytoplankton biomass and size structure to estimate export of both algal aggregates and zooplankton fecal pellets out of the surface ocean. For details on the satellite data products used to drive the surface module, see Siegel et al. (2014). The twilight zone module tracks the fate of exported carbon in the mesopelagic and adds the effects of zooplankton DVM. The twilight zone component is vertically structured and defines the depth dependence of the vertical flux of particulate organic carbon (POC) and the production of respiratory dissolved inorganic carbon (DIC), or equivalently, oxygen consumption. A description of each model state variable and the associated units are listed in Table 1.

Export out of the euphotic zone is modeled here as the sum of two separate fluxes, the passive sinking flux (F_{eu}) and the DVM-mediated flux (J_{dvm}).

$$\text{Total Export Flux} = F_{eu} + J_{dvm} \tag{1}$$

F_{eu} is defined as the sum of the sinking of phytoplankton cell aggregates (F_{alg}) and the sinking of zooplankton fecal pellets produced in the euphotic zone (F_{fec}).

$$F_{eu} = F_{alg} + F_{fec} \tag{2}$$

J_{dvm} is the sum of fecal pellets produced in the twilight zone (J_{fec}) and carbon metabolized by migrating zooplankton in the twilight zone (J_{met}).

$$J_{dvm} = J_{fec} + J_{met} \tag{3}$$

2.1.1. The Euphotic Zone Module

The drivers of the food web model in the euphotic zone are satellite-derived monthly climatologies of NPP and phytoplankton biomass in two size classes, nanophytoplankton and microphytoplankton (P_n, P_m), from the Sea-viewing Wide-Field-of-view Sensor ocean color mission (Siegel et al., 2014). The model assumes that

Table 1
Model State Variables

Variable	Description	Units
F_{eu}	total POC flux out of the euphotic zone	mgC·m^{-2}·day^{-1}
J_{dvm}	DVM-mediated export flux	mgC·m^{-2}·day^{-1}
F_{alg}	flux of algal aggregates out of the euphotic zone	mgC·m^{-2}·day^{-1}
F_{fec}	flux of fecal pellets out of the euphotic zone	mgC·m^{-2}·day^{-1}
J_{fec}	flux of fecal pellets produced in twilight zone	mgC·m^{-2}·day^{-1}
J_{met}	metabolized carbon produced in twilight zone	mgC·m^{-2}·day^{-1}
P_n	nanophytoplankton biomass	mgC/m^3
P_m	microphytoplankton biomass	mgC/m^3
NPP_m	microphytoplankton NPP	mgC·m^{-2}·day^{-1}
NPP_n	nanophytoplankton NPP	mgC·m^{-2}·day^{-1}
G_m	grazing rate on microphytoplankton	mgC·m^{-3}·day^{-1}
G_n	grazing rate on nanophytoplankton	mgC·m^{-3}·day^{-1}
z_{eu}	depth of the euphotic zone	m
z_{ml}	depth of the mixed layer	m
G_{abs}	grazed carbon absorbed by zooplankton	mgC·m^{-3}·day^{-1}
Z	zooplankton biomass	mgC/m^3
z_{iso}	depth of the 10^{-3}-W/m^2 isolume	m
$F(z)$	POC flux in the twilight zone	mgC·m^{-3}·day^{-1}
$T(z)$	temperature	°C
$O_2(z)$	dissolved oxygen concentration	μmol/L
$R(z)$	time rate of change of DIC in the twilight zone	mgC·m^{-3}·day^{-1}

Note. POC = particulate organic carbon; NPP = net primary production; DVM = diel vertical migration; DIC = dissolved inorganic carbon.

a fixed proportion (f_{alg}) of the NPP fraction produced by microphytoplankton integrated over the euphotic zone (NPP_m) is exported as sinking aggregates such that

$$F_{alg} = f_{alg} NPP_m \tag{4}$$

None of the NPP fraction from nanophytoplankton (NPP_n) is exported as sinking aggregates. The value of f_{alg} is assumed to be 0.1 based on previous food web models (Boyd et al., 2008; Michaels & Silver, 1988; Siegel et al., 2014). Fecal pellet production depends on zooplankton grazing, where the volumetric rate of grazing on each phytoplankton class (G_n, G_m) is estimated using a food web model forced by measurements of NPP and the time rate of change in phytoplankton biomass (Siegel et al., 2014).

$$\frac{dP_i}{dt} = \frac{NPP_i}{z_{eu}} - G_i - \delta_i \frac{F_{alg}}{z_{eu}} - m_p P_i - \frac{P_i}{z_{ml}} \frac{dz_{ml}}{dt} H\left(\frac{dz_{ml}}{dt}\right) \tag{5}$$

dP_i/dt is the observed time rate of change of the ith size fraction of phytoplankton biomass, NPP_i is the vertically integrated NPP of each phytoplankton size fraction, G_i is the grazing rate on each size fraction of phytoplankton, z_{eu} is the euphotic depth, and m_p is the linear mortality rate of phytoplankton. The phytoplankton linear mortality rate is equal to 0.1 day^{-1} following previous model parameterizations (Moore et al., 2004; Siegel et al., 2014). Because the sinking flux loss term, F_{alg}/z_{eu}, only affects microphytoplankton, $\delta_i = 1$ when $i = m$ and $\delta_i = 0$ when $i = n$. The final term in equation (5) is the detrainment term, which represents dilution when the mixed layer is deepening such that $H(x) = 1$ if $x > 0$ and 0 otherwise (Siegel et al., 2014).

The estimated grazing rates on the nanosize and microsize fraction of NPP support the growth of small and large zooplankton, respectively (Figure 1). Large zooplankton also graze on small zooplankton. In this model, "large zooplankton" refers to those organisms which spend some portion or all of their diel cycle in the euphotic zone. It does not include zooplankton that are residents of the twilight zone and never cross

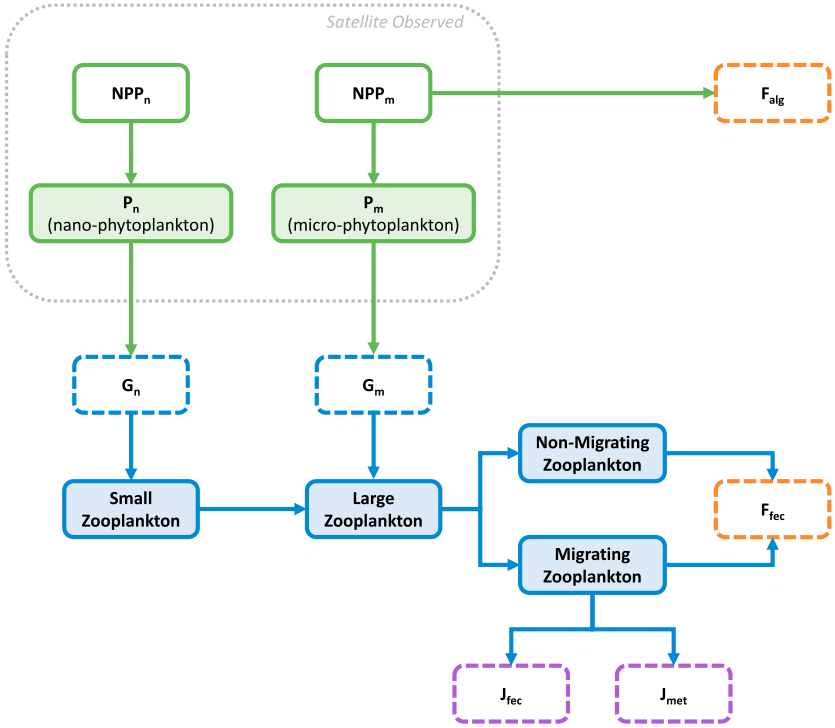

Figure 1. Conceptual diagram of the plankton food web as represented in the model and including the various export fluxes. Biomass standing stocks are indicated by solid lines and fluxes by dashed lines. Orange indicates a passive sinking export flux out of the euphotic zone, and purple indicates diel vertical migration-mediated fluxes. The gray dashed line shows values that are empirical observations derived from satellite data products. NPP = net primary production.

the euphotic zone boundary. A portion of the total grazing flux into the large zooplankton box is converted to sinking fecal pellets, which includes both direct grazing on microphytoplankton and indirect grazing on nanophytoplankton through grazing on small zooplankton. The fraction of large zooplankton fecal pellets that are produced in the euphotic zone and the twilight zone, respectively, will depend on the fraction of the large zooplankton community that is participating in DVM and the proportion of fecal pellets produced in the euphotic zone by migrating zooplankton. The fecal pellet flux out of euphotic zone (F_{fec}) is estimated as

$$F_{\mathrm{fec}} = (p_{\mathrm{dvm}} f_{\mathrm{fec}} + (1 - p_{\mathrm{dvm}}))(m_{\mathrm{fec}} G_m + n_{\mathrm{fec}} G_n) z_{\mathrm{eu}} \tag{6}$$

and those fecal pellets not produced in the euphotic zone are carried by migrating zooplankton to the twilight zone. Fecal pellets produced in the twilight zone by migrators from the surface (J_{fec}) are modeled as

$$J_{\mathrm{fec}} = p_{\mathrm{dvm}} (1 - f_{\mathrm{fec}})(m_{\mathrm{fec}} G_m + n_{\mathrm{fec}} G_n) z_{\mathrm{eu}} \tag{7}$$

where G_m and G_n are the volumetric grazing rates on microphytoplankton and nanophytoplankton, respectively, m_{fec} and n_{fec} are the proportion of grazed carbon on each phytoplankton size class converted to large zooplankton fecal pellets, p_{dvm} is the fraction of large zooplankton in the euphotic zone participating in DVM, and f_{fec} is the fraction of fecal pellets produced in the euphotic zone. The conversion of nanophytoplankton biomass into large zooplankton fecal pellets is significantly less efficient due to the extra trophic step through small zooplankton, so we set m_{fec} equal to 0.3 and n_{fec} equal to 0.1 based on previous modeling studies (Michaels & Silver, 1988; Siegel et al., 2014). Observations of DVM biomass, based on the zooplankton biomass difference between day and night, indicate that the fraction of the zooplankton community participating in DVM can vary greatly and ranges from near 0 to near 1 based on season and size fraction (Isla et al., 2015; Putzeys & Hernandez-Leon, 2005; Takahashi et al., 2009). Analysis of acoustic scattering layer data by Klevjer et al. (2016) found that an average of 50% of the mesopelagic backscatter participated in DVM, although this number varied significantly between different oceanographic regions and ranged from 20% to 90%. We assumed a global value for p_{dvm} of 0.5 based on these results.

The fraction of fecal pellets produced in the euphotic zone by migrating zooplankton depends on the time that migrating zooplankton spend in the euphotic zone relative to their gut clearance rate. The timing of DVM corresponds well to sunrise and sunset (Bianchi & Mislan, 2016), so we have assumed that the time that migrating zooplankton spend in the twilight zone is equal to day length. Based on evidence that grazing rates for migrating zooplankton are most intensive during the night (Haney, 1988), we assumed that all grazing by vertically migrating zooplankton occurs in the euphotic zone rather than the twilight zone. The only fecal pellets that are produced at depth are the result of one gut-full brought down from the surface. Therefore, the fraction of fecal pellets that migrating zooplankton produce in the twilight zone is equal to the ratio of one gut-full of grazed phytoplankton biomass to the total number of gut-fulls grazed over the daytime portion of the light cycle. Therefore, f_{fec} is defined as

$$f_{\mathrm{fec}} = 1 - \frac{r}{\text{24-day length}} \tag{8}$$

where r is the mean gut clearance rate for grazing zooplankton and day length is represented as a function of latitude and day of the year following Forsythe et al. (1995). There is considerable variability among measurements of zooplankton gut clearance rates resulting from differences in taxa, body size, life history stage, and temperature, with estimates ranging from 20 to 100 min (Atkinson et al., 1996; Bautista & Harris, 1992; Dam & Peterson, 1988). Clearance rates also tend to be slower for zooplankton participating in DVM (Atkinson et al., 1996). Here, we have chosen to use a constant value for gut clearance rate of 1 hr. Equation (8) will fail to accurately represent the time fraction that migrating zooplankton spend in the euphotic zone when day length approaches either 0 or 24 hr, such as occurs near the poles, when DVM timing may not reflect the length of the solar day (Fischer & Visbeck, 1993; Last et al., 2016). However, due to constraints on available satellite data as discussed below, the analysis of this model was restricted to the area between 60°N and 60°S.

Grazed carbon, which is not converted into fecal pellets, is absorbed by zooplankton to be either metabolized or assimilated into biomass. It is important to note that we only modeled large zooplankton explicitly and then only those large zooplankton, which spend some part of their diel cycle in the euphotic zone, since small zooplankton were assumed to not participate in DVM (Isla et al., 2015). The absorbed carbon is the fraction of grazed phytoplankton biomass, which is converted into large zooplankton biomass. Similar to the conversion of phytoplankton biomass to fecal pellets discussed above, the conversion of phytoplankton biomass to large zooplankton biomass is thought to be more efficient for the microsize fraction than the nanosize fraction because of the additional trophic step through small zooplankton. We scaled the conversion of grazed nanophytoplankton into large zooplankton by the ratio of $n_{\mathrm{fec}} : m_{\mathrm{fec}}$ to reflect the loss of organic carbon from small zooplankton respiration prior to consumption by large zooplankton. Grazed carbon absorbed by large zooplankton (G_{abs}) is calculated as

$$G_{\mathrm{abs}} = (1 - m_{\mathrm{fec}})G_m + \frac{n_{\mathrm{fec}}}{m_{\mathrm{fec}}}(1 - m_{\mathrm{fec}})G_n \tag{9}$$

A fixed proportion of the carbon absorbed by large zooplankton is respired and the relative proportion of this respiration which occurs in the twilight zone is based on the temperature difference between the surface and a given depth. J_{met}, the production of respiratory DIC in the twilight zone by vertically migrating zooplankton, is given by

$$J_{\mathrm{met}} = p_{\mathrm{met}} p_{\mathrm{dvm}} (f_{\mathrm{met}} G_{\mathrm{abs}} z_{\mathrm{eu}}) \tag{10}$$

where

$$p_{\mathrm{met}} = \frac{Q_{10}^{\frac{T(z)-T(0)}{10}}}{Q_{10}^{\frac{T(z)-T(0)}{10}} + 1} \tag{11}$$

f_{met} is the fraction of absorbed carbon that is metabolized, p_{met} is the fraction of total metabolism that occurs in the twilight zone, Q_{10} is the metabolic temperature coefficient, $T(z)$ is the temperature at depth z, and $T(0)$ is the temperature at the surface. We set f_{met} equal to 0.5 and Q_{10} equal to 2 (Ikeda, 2014; Steinberg & Landry, 2017).

Large zooplankton biomass in the euphotic zone (Z) was modeled as

$$\frac{dZ}{dt} = (1 - f_{met})G_{abs} - m_z(Z - Z_0) - p_z(Z - Z_0)^2 \quad (12)$$

where m_z and p_z are linear and quadratic mortality rates, respectively, and Z_0 is a lower threshold for zooplankton biomass, which was included to stabilize the model. We chose values of 0.05 day^{-1} for m_z and 0.15 $mgC^{-1}{\cdot}m^3{\cdot}d^{-1}$ for p_z to be consistent with previous models of surface food webs (Doney et al., 1996; Fasham et al., 1990). This equation is implemented with $Z(t)$ as a state variable that changes dynamically in time over a climatological seasonal cycle at each grid location.

2.1.2. The Twilight Zone Module

We assumed that migrating zooplankton in the twilight zone were normally distributed about a mean migration depth located at the 10^{-3}-W/m^2 isolume (Bianchi, Stock, et al., 2013). We parameterized the variability in zooplankton DVM depth with a truncated Gaussian function that was 100 m wide and had a half power thickness of 50 m based on acoustic measurements of the thickness of the migrating zooplankton layer in DVM events by Bianchi and Mislan (2016). The depth of this isolume is calculated using satellite measurements of surface photosynthetically active radiation (PAR) and two separate light attenuation coefficients (k), one for the euphotic zone and one for the twilight zone. The PAR attenuation coefficient in the euphotic zone was calculated from satellite-observed euphotic depth, where the variable z_{eu} is defined as the depth at which PAR is 1% of the measured surface value. The value of k for the twilight zone was set to 0.03 based on minimum in situ light attenuation measurements (Son & Wang, 2015). The depth of migration was further restricted by in situ oxygen concentration. We defined the lower limit of zooplankton hypoxia tolerance as 15 μmol/L. The mean depth of migration is then the shallower depth of the 10^{-3}-W/m^2 isolume and the 15-μmol/L oxygen isopleth.

Large zooplankton fecal pellets produced in the twilight zone (J_{fec}) contribute to the sinking POC flux composed of algal aggregates and zooplankton fecal pellets produced in the euphotic zone. We assumed that the gut clearance rate and the migration transit time were roughly equivalent based on global estimates of the mean transit time (1.75 hr) from acoustic data (Bianchi & Mislan, 2016). Fecal pellets carried by vertical migrators were distributed along the migration path using a uniform distribution between the euphotic depth and the maximum migration depth to produce a depth-dependent function of fecal pellet production in the twilight zone ($J_{fec}(z)$). In contrast, we assume that the migration transit time is small compared to the time spent at depth such that DIC produced by migrating zooplankton in the twilight zone is centered around the maximum migration depth rather than distributed along the migration path. We calculated the depth-dependent distribution of the production of metabolic DIC around the amaximum migration depth ($J_{met}(z)$) by taking the convolution of J_{met} with the truncated Gaussian described above that represents variability in the concentration of migrating zooplankton around the target depth.

The shape of the POC flux profile in the euphotic zone results from the combined influence of physical and biological factors including the breakage of large particles into smaller slower-sinking ones, remineralization by the attached microbial community, and grazing by mesopelagic (nonmigrating) zooplankton and fish, all of which serve to attenuate the flux over depth, and the influx of fecal pellets produced by migrating large zooplankton, which adds to the flux. We parameterized the physical and biological attenuation of the POC flux as the exponential decay of the labile portion of the flux and included the effect of temperature and dissolved oxygen concentration on the remineralization rate (Laufkötter et al., 2017; Lima et al., 2014). The POC flux profile in the twilight zone ($F(z)$) was discretized as a function of depth such that

$$F(z_i) = (1 - \alpha)F(z_{i-1}) + \alpha F(z_{i-1}) \exp[\frac{-1}{\lambda} e^{k_t T(z_i)} \frac{O_2(z_i)}{O_2(z_i) + k_o} \Delta z] + J_{fec}(z_i) \quad (13)$$

with upper boundary condition $F(z_{eu}) = F_{eu}$. Algorithmically, this means that at each depth bin we apply the exponential decay function to the influx of sinking particles from the depth bin above plus the input of fecal pellets from $J_{fec}(z)$. Δz is the depth bin width, α is the labile fraction of the flux, λ is the characteristic length scale of remineralization, k_t is the temperature dependence parameter, and k_o is the oxygen half-saturation coefficient. The characteristic length scale is defined as the ratio of sinking speed (m/day) to remineralization rate (1/day). Within a temperature dependent parameterization, λ is the characteristic length scale at 0 °C where the temperature coefficient is 1. While the reference λ remains constant, the remineralization length scale is modulated by the temperature dependence term such that the functional length

Table 2
Model Parameters

Parameter	Description	Value	Units
f_{alg}	fraction of NPP_m exported as aggregates	0.1	
m_p	phytoplankton linear mortality	0.1	day^{-1}
p_{dvm}	fraction of zooplankton vertically migrating	0.5	
m_{fec}	fraction of grazed NPP_m converted to fecal pellets	0.3	
n_{fec}	fraction of grazed NPP_n converted to fecal pellets	0.06	
f_{fec}	fraction of fecal pellet production in the euphotic zone	var.	
r	gut clearance rate	1	hr
p_{met}	fraction of metabolism in the twilight zone	var.	
Q_{10}	Q_{10} temperature coefficient	2	
f_{met}	fraction of absorbed carbon metabolized	0.5	
m_z	zooplankton linear mortality	0.05	day^{-1}
p_z	zooplankton quadratic mortality	0.01	$mgC^{-1}{\cdot}m^3{\cdot}day^{-1}$
k	PAR attenuation coefficient	0.03	m^{-1}
α	biomass labile fraction	0.8	
λ	remineralization length scale	200	m
k_t	remineralization temperature dependence	0.05	$°C^{-1}$
k_o	oxygen half-saturation coefficient	10	μmol/L
Δz	depth interval	10	m

Note. NPP = net primary production; PAR = photosynthetically active radiation.

scale is equal to 200 m at 0 °C and declines to 200/e m at 20 °C. The parameter values for this function (Table 2) are consistent with previous models of mesopelagic remineralization of the POC flux (Laufkötter et al., 2017; Lima et al., 2014). We used 2009 World Ocean Atlas data (annual climatology, 1° grid) to define the mesopelagic temperature ($T(z)$, °C) and oxygen concentrations (O_2, μmol/L).

Oxygen consumption and the production of metabolic DIC in the model is the sum of remineralization of the vertical POC flux and the metabolism of vertically migrating zooplankton. The respiratory source term ($R(z)$), or equivalently the transformation of organic carbon in the euphotic zone to DIC in the twilight zone, is defined as

$$R(z) = \frac{\mathrm{dDIC}}{\mathrm{d}t} = -\frac{\mathrm{d}F}{\mathrm{d}z} + J_{\mathrm{met}}(z) \tag{14}$$

We defined three metrics to quantify the relative contributions of model variables to water column biogeochemistry. The DVM export ratio is the ratio of the DVM-mediated export flux to the total export flux to below the euphotic zone,

$$\text{DVM Export Ratio} = \frac{J_{\mathrm{dvm}}}{J_{\mathrm{dvm}} + F_{\mathrm{eu}}} \tag{15}$$

Similarly, the DVM respiration ratio is the ratio of the respiration performed by vertically migrating zooplankton to the integrated respiration in the mesopelagic from the euphotic depth to 1,000 m.

$$\text{DVM Respiration Ratio} = \frac{J_{\mathrm{met}}}{\int_{z_{\mathrm{eu}}}^{1{,}000} R(z)\mathrm{d}z} \tag{16}$$

Finally, we defined the weighted depth of respiration to quantify how DVM activity by zooplankton pushes the production of DIC and oxygen utilization deeper into the water column.

$$\text{Weighted Depth of Respiration} = \frac{\int_{z_{\mathrm{eu}}}^{1{,}000} z * R(z)\mathrm{d}z}{\int_{z_{\mathrm{eu}}}^{1{,}000} R(z)\mathrm{d}z} \tag{17}$$

Because the weighted depth of respiration depends on both DVM activity and variability in the temperature and oxygen concentrations, we report the "Respiration Depression" as the difference between the weighted depth of respiration from the DVM model and a baseline remineralization profile that includes only the respiration of sinking particles and no DVM ($p_{dvm} = 0$).

Together these metrics quantify the magnitude of the effect that zooplankton DVM has on carbon export out of the euphotic zone and on DIC production and oxygen utilization in the twilight zone. Higher values of the DVM export ratio and the DVM respiration ratio indicate that zooplankton migrations are accounting for greater fractions of carbon export and oxygen utilization in the twilight zone. A positive value of the respiration depression indicates that zooplankton DVM is pushing the DIC production and oxygen utilization deeper in the water column.

2.2. Application of the Model

We first applied the above one-dimensional model to monthly mean satellite observations from the Bermuda Atlantic Time Series (BATS) scientific station at 31°40′N, 64°10′W. We calculated the depth profile of the vertical POC flux and the profile of DIC production in the twilight zone, and the export ratio over the seasonal cycle (total carbon export out of the euphotic zone divided by depth-integrated NPP). For this test case, and in contrast to the global model discussed below, the mean and SD calculated for this grid point represents seasonal variability over monthly means from the annual climatology and does not account for regional variability.

Next, we applied the one-dimensional model to a global, 1° grid. We kept the parameters of the model constant across the global domain. These parameter estimates represent mean or characteristic values that describe a variety of different phytoplankton and zooplankton communities which occur in the world's oceans. Differences between grid points are the result of variability in the drivers of the model—observed NPP, phytoplankton biomass, size structure, temperature, and oxygen concentration. A baseline simulation was run with $p_{dvm} = 0$ for a control scenario in which there was no DVM. Global patterns were based on the annual mean over the seasonal cycle at each grid point. The mean and SD calculated for the global model includes both seasonal and regional variability. Only grid points that had at least 8 months of available satellite data over the seasonal cycle were included in the analysis. This excluded most of the grid at high latitudes due to the persistence of clouds and sea ice cover, and the extended duration of the polar night.

We tested the sensitivity of the model to each of the parameters numerically by increasing each of the parameters by 1% and calculating the resulting change in a suite of model outputs that serve to characterize the magnitude and composition of the global export flux: the total global export flux, the average export ratio, the average magnitude of the passive sinking flux, the average magnitude of the DVM-mediated export flux, the DVM export ratio, the DVM respiration ratio, and the respiration depression. The choice of a 1% perturbation is not intended to reflect realistic estimates of parameter error but, instead, is used as a baseline to test the relative sensitivity of the model to each parameter. A response close to or greater than 1% (in either the positive or negative direction) indicates a relatively high sensitivity to that parameter. The assumption implicit to this approach is that parameter error falls within a region of linear stability. We tested the model response to parameter perturbations of up to 100% and confirmed that the sensitivity is linear for most model parameters and outputs, indicating the sensitivity results presented here should scale well with parameter errors larger than 1%.

3. Results

3.1. 1-D Model at BATS

Annual mean (± SD) NPP at the BATS grid point was 277 ± 58 mgC·m^{-2}·day^{-1}. Satellite climatologies of phytoplankton biomass show a seasonal mixed layer phytoplankton bloom dominated by nanophytoplankton with peaks in March and September (Figure 2). Microphytoplankton biomass was low over the entire seasonal cycle, with a small increase in February, just before the nanophytoplankton bloom. During the summer, when nanophytoplankton biomass was high, microphytoplankton biomass was near 0. Modeled large zooplankton biomass was lower than phytoplankton biomass and showed significantly less seasonality. A small peak in zooplankton occurred during March and April following the increase in microphytoplankton. The mean (± SD) nanophytoplankton biomass was 10 ± 2.7 mgC/m^3, mean microphytoplankton biomass was 0.8 ± 0.79 mgC/m^3, and mean zooplankton biomass was 3.5 ± 0.7 mgC/m^3. Mean euphotic depth at

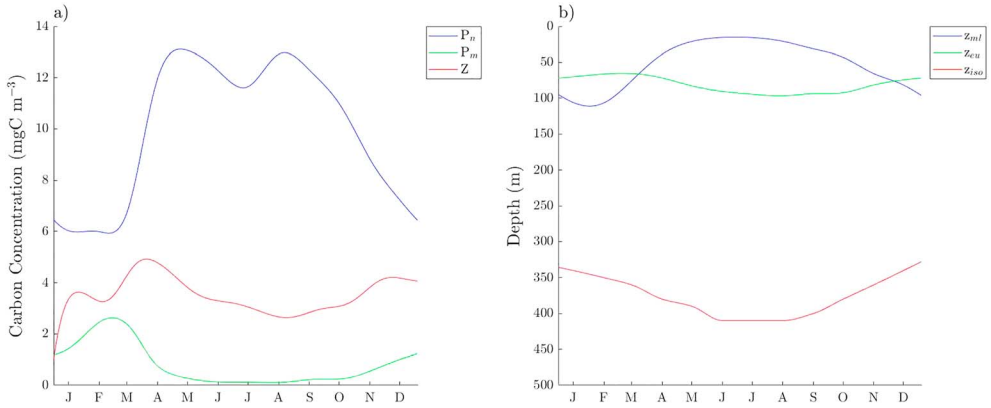

Figure 2. (a) Biomass of nanophytoplankton and microphytoplankton (P_n, P_m) and zooplankton (Z) in the mixed layer over the seasonal cycle at the Bermuda Atlantic Time Series grid point. (b) Depth of the euphotic zone (z_{eu}), the mixed layer (z_{ml}), and the 10^{-3}-W/m^2 isolume (z_{iso}).

BATS was 82 ± 11 m, mean mixed layer depth was 52 ± 33 m, and mean depth of the 10^{-3}-W/m^2 isolume was 378 ± 27 m (Figure 2).

Figure 3 shows the monthly averages of the magnitude of the carbon export fluxes F_{eu} and J_{dvm} at BATS, as well as the quantitative metrics used to evaluate the relative magnitude of these fluxes. Export from the euphotic zone by passive sinking (F_{eu}) showed significant seasonality with a peak in March and April corresponding to the yearly maximum in microphytoplankton and zooplankton biomass. F_{eu} was dominated by the sinking fecal pellet flux. J_{dvm} is approximately one third as large as F_{eu} and, in contrast, is dominated by metabolic production of DIC in the twilight zone rather than fecal pellets. Model estimates of the export ratio, DVM export ratio, and the DVM respiration ratio showed very little seasonality. The mean (± SD) export ratio at BATS was 0.07 ± 0.03, with an annual mean fraction of 0.05 of the NPP exported by F_{eu} and 0.02 by J_{dvm}. The annual mean DVM export ratio was 0.23 ± 0.02 and the annual mean DVM respiration ratio was 0.21 ± 0.02, indicating that zooplankton DVM activity accounted for approximately equal proportions of total export and total twilight zone respiration. The annual mean respiration depression, compared to the model run which did not account for DVM, was 54 ± 8 m. Respiration depression showed significant seasonality with much larger values in the summer than in the winter.

Figure 4 shows the depth dependence of the vertical POC flux and the production of DIC, or equivalently, oxygen utilization in the twilight zone at BATS. While DVM activity is responsible for a large local maximum in DIC production at depth, it has relatively little impact on the vertical profile of sinking POC because the magnitude of J_{fec} is much smaller than J_{met} and because fecal pellets are deposited uniformly along the migration path and DIC is all produced at the maximum depth. In the absence of any DVM behaviors, the profiles of both POC flux and DIC production would be monotonically decreasing (Figure 4).

3.2. Global Model Dynamics

Annual mean (± SD) global NPP was 414 ± 194 mgC·m^{-2}·day^{-1}, with an integrated global carbon flux of 6.5 PgC/year. The global mean export ratio was 0.12 ± 0.05. Passive sinking of particles out of the euphotic zone (F_{eu}) accounted for an annual mean (± SD) fraction of 0.1 ± 0.05 of the global NPP and the DVM-mediated flux (J_{dvm}) accounted for an additional 0.02 ± 0.01 of global NPP. The carbon transported by zooplankton DVM was a significant contributor to the export flux. In the control run with no DVM, the global carbon export flux was 5.7 PgC/year and the annual mean export ratio was 0.10 ± 0.04. The integrated global flux values represent an area of the ocean that is 3.16 × 10^8 km^2, which is approximately 20% smaller than the total area of the ocean (Siegel et al., 2014). Due to constraints on available data for grid points found at high latitudes, polar blooms are largely absent from these calculations.

The global distributions of model drivers and state variables are shown in Figure 5. NPP is higher near the coast and in upwelling zones, including eastern boundaries and around the equator. The high NPP areas tend to be dominated by microphytoplankton, while nanophytoplankton dominate the ecosystem in the center of ocean gyres in the subtropical latitudes. Modeled large zooplankton biomass had similar patterns to NPP. The global mean (± SD) zooplankton biomass was 2.8 ± 0.9 mgC/m^3. The mean DVM depth was

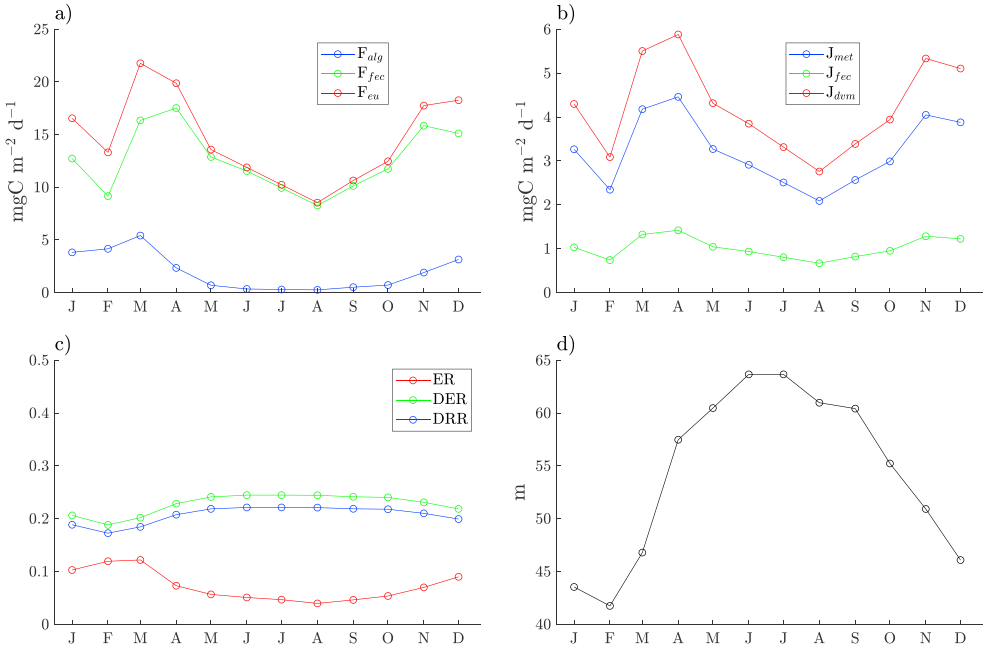

Figure 3. Monthly means of (a) the passive sinking flux (F_{eu}); (b) the DVM-mediated export flux (J_{dvm}); (c) the export ratio (ER), DVM export ratio (DER), and the DVM respiration ratio (DRR); and (d) respiration depression at Bermuda Atlantic Time Series. Note the difference of vertical scales between (a) and (b). DVM = diel vertical migration.

356 ± 41 m. Migration depth was typically deeper in the subtropics where incident light is high and chlorophyll concentrations are low, although mesopelagic oxygen concentration had a strong shoaling effect. Large hypoxic regions, such as the north and south subtropical eastern Pacific and the northern Indian Ocean had migration depths significantly lower than the global mean. The modeled migration depths were only slightly shallower, on average, than the global mean DVM depth reported by Bianchi and Mislan (2016), who estimated a mean value of 411 m based on acoustic Doppler current profiler data from 1990 to 2010. This discrepancy may indicate that modeling migration depth by assuming a constant target isolume modified by low oxygen concentrations may be insufficient.

The magnitude of the total export flux, as well as each of the component fluxes F_{eu} and J_{dvm}, was larger in highly productive coastal zones and upwelling regions (Figure 6). However, despite the magnitude of these fluxes following patterns in NPP, the relative contribution of F_{eu} and J_{dvm} to total export displayed distinctly different global patterns (Figure 7). Both the DVM export ratio and the DVM respiration ratio, which define the proportional contributions of DVM activity to total export and mesopelagic respiration, were higher in the subtropical latitudes where the community was dominated by nanophytoplankton (Figure 5). Respiration depression was highest in the subtropical latitudes as well, with significantly reduced values in hypoxic regions where the migration depth was very shallow (Figure 7). The global mean (± SD) DVM export ratio was 0.16 ± 0.04. The global mean DVM respiration ratio was 0.16 ± 0.06. The global mean respiration depression was 30 ± 18 m. A summary of the global results is presented in Table 3.

3.3. Model Sensitivity

We tested sensitivity by calculating the model response to a 1% change in each of the parameters. Proportional responses close to or greater than 1% indicate a relatively high sensitivity to a given parameter. All of the model responses fell between −2% and +1%. The modeled total global export flux was more robust to changes in the parameter values than the relative contributions of F_{eu} and J_{dvm} to total export (Figure 8). The global export flux was most sensitive to n_{fec}, which controls the fraction of grazed phytoplankton biomass in the nanosize class that is converted into large zooplankton fecal pellets. Importantly, the relative value of n_{fec} to m_{fec} also parameterizes the trophic efficiency of large zooplankton grazing on nanophytoplankton indirectly through the consumption of small zooplankton, and so n_{fec} also plays a role in determining how much total phytoplankton biomass is absorbed by large zooplankton and, ultimately, how much carbon is respired by vertically migrating zooplankton. The relative contributions of F_{eu} and J_{dvm} to total export—quantified

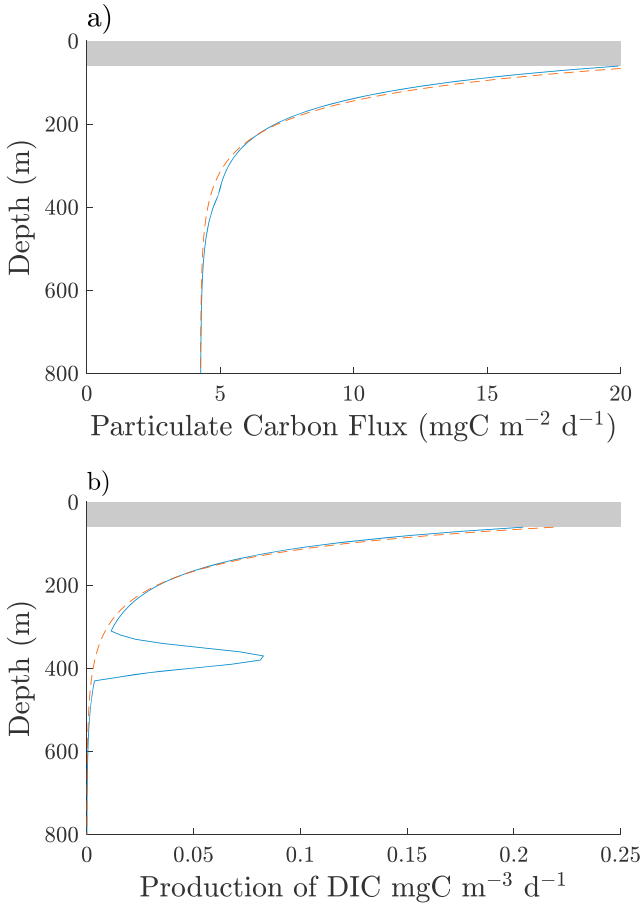

Figure 4. Vertical profiles at Bermuda Atlantic Time Series of (a) particulate carbon flux ($F(z)$) and (b) the production of DIC ($R(z)$) in the twilight zone for the month of April, during the peak of the phytoplankton bloom. The euphotic zone is indicated by the gray box. The blue line represents a model run when $p_{\mathrm{dvm}} = 0.5$, and the red dashed line represents the control run when $p_{\mathrm{dvm}} = 0$. DIC = dissolved inorganic carbon.

by the DVM export ratio, the DVM respiration ratio, and the respiration depression—were all most sensitive to f_{fec}, p_{dvm}, and f_{met}. These three parameters do not determine the total amount of carbon exported but contribute heavily to determining the partitioning of exported carbon between passive sinking and active transport pathways.

4. Discussion

We approached the challenge of modeling DVM by assuming general principles and parameters for the pelagic ecosystem that were applied globally. Neither model formulation nor parameter values were changed across the model domain. Instead, variability in the inputs (NPP, phytoplankton biomass, and size structure) was the drivers of the system rather than regional differences in ecosystem description. This conceptual approach allowed us to work around the problem of incomplete knowledge concerning regional differences in the plankton community and provides a blueprint for future work. Model estimates of the global carbon export flux (6.5 PgC/year) are consistent with recent model estimates of the global surface POC flux ranging from 5 to 12 PgC/year (Siegel et al., 2016). The flux of carbon to below the euphotic zone mediated by zooplankton DVM is an important part of the biological pump, increasing the global export flux by 14%.

The one-dimensional model run at the BATS grid point provides a case study, which can be used to evaluate the performance of the model in the subtropics, a region where the effect of DVM activity on carbon export and mesopelagic biogeochemistry is significant. Overall, the model does a reasonable job of representing the biological pump at BATS considering the model was designed to represent a generalized global ecosystem and was not specifically parameterized for the BATS location. Satellite climatologies of

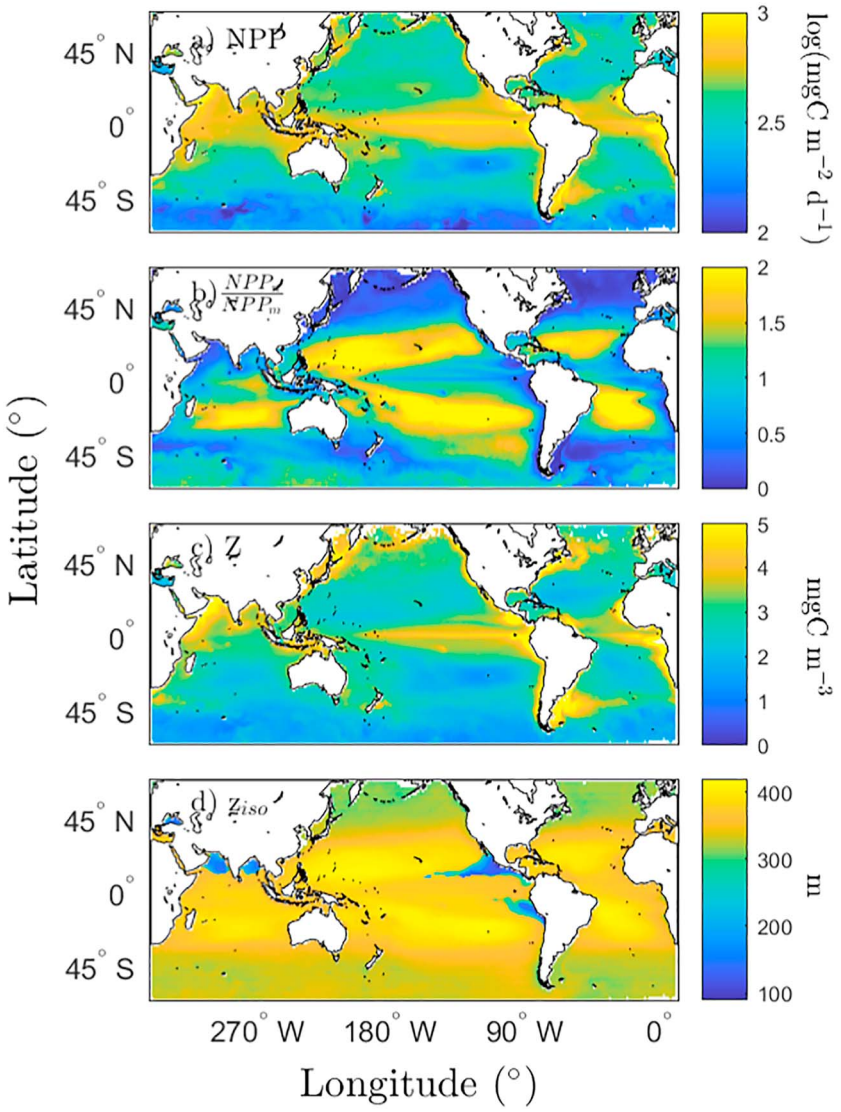

Figure 5. Global distribution of (a) net primary productivity (NPP), (b) the NPP biovolume ratio (NPP_n/NPP_m), (c) zooplankton biomass (Z), and (d) migration depth (z_{iso}). The value at each grid point is the annual mean over the seasonal cycle.

production and phytoplankton biomass are consistent with long-term in situ measurements at the BATS station (Steinberg et al., 2001). Both satellite observations and in situ measurements show a succession from larger diatom cells in the early spring to a more diverse community of smaller cells that dominate during the summer. However, significant differences are found between the model estimates of mean large zooplankton biomass integrated over the euphotic zone (3.5 ± 0.7 mgC/m^3) and in situ measurements made at BATS. Madin et al. (2001) measured zooplankton biomass in the top 200 m from 1994 to 1998 and estimated a mean value of 1.16 ± 0.19 mgC/m^3. The discrepancy between model estimate and observation could indicate that the zooplankton mortality terms are poorly defined for this location. However, the general lack of strong seasonal patterns in zooplankton biomass, besides the small peak in early spring, was consistent with observations (Madin et al., 2001; Steinberg et al., 2001). Model estimates of the mean total export flux (18.8 mgC·m^{-2}·day^{-1}) and the mean export ratio (0.07) at BATS were reasonable compared to long-term measurements made at the time series location from 1989 to 1997, where Steinberg et al. (2001) report mean values of 25.8 mgC·m^{-2}·day^{-1} and 0.06, respectively. Table 4 provides a summary of these comparisons.

We also compared the modeled large zooplankton biomass across the global domain to estimates of global mesozooplankton biomass made by Moriarty and O'Brien (2013) using the Coastal and Oceanic Plankton

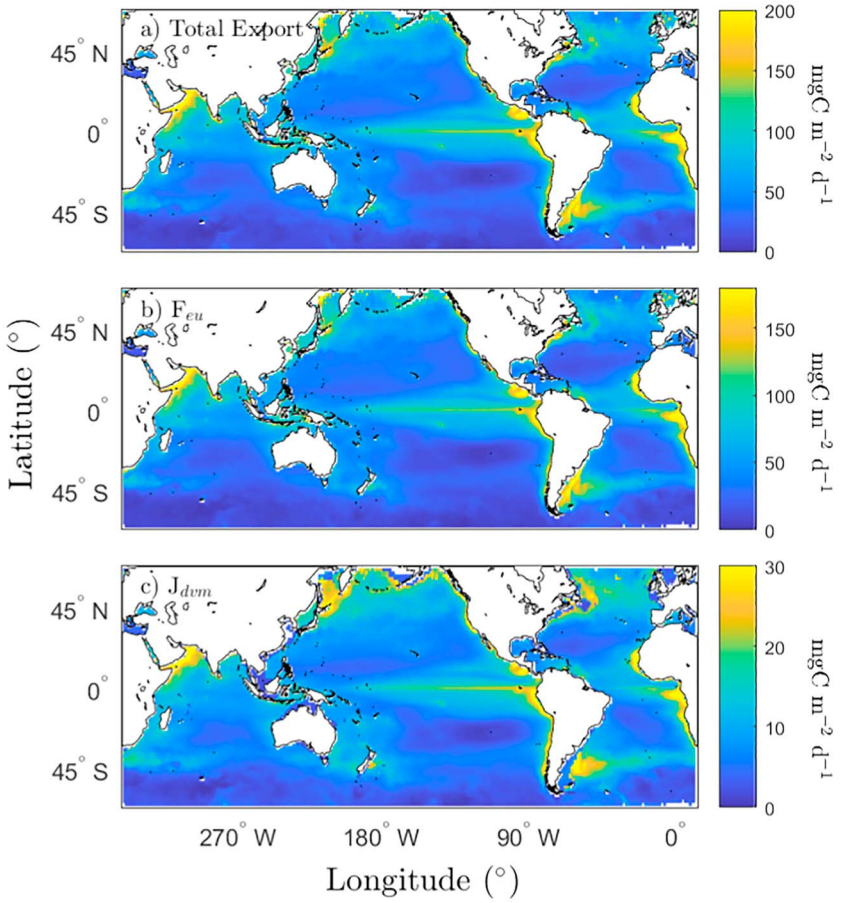

Figure 6. Global distribution of the magnitude of the (a) total export flux, (b) the passive sinking export flux (F_{eu}), and (c) the DVM-mediated export flux (J_{dvm}). The value at each grid point is the annual mean over the seasonal cycle. DVM = diel vertical migration.

Ecology, Production, and Observation Database (COPEPOD). The COPEPOD database combines mesozooplankton biomass measurements from 110 studies and converts the data to reflect the 333-μm mesh size fraction over the depth range from 0 to 500 m. The model predicts a global mean large zooplankton biomass of 2.8 mgC/m^3 with a SD of 0.9 mgC/m^3, while COPEPOD has a global mean of 5.9 mgC/m^3, a median of 2.7 mgC/m^3, and a SD of 10.6 mgC/m^3 (Moriarty & O'Brien, 2013). We can infer from this comparison that the model does a good job of describing the central tendency of the global distribution of zooplankton

Table 3
Summary of Global Statistics

Statistic	Mean (SD)	
	$p_{dvm} = 0$	$p_{dvm} = 0.5$
NPP (mgC·m^{-2}·day^{-1})	414 (194)	414 (194)
Global export flux (PgC/year)	5.7	6.5
Export ratio	0.10 (0.04)	0.12 (0.05)
DVM export ratio		0.16 (0.04)
DVM respiration ratio		0.16 (0.06)
Respiration depression (m)		30 (18)

Note. Annual mean and standard deviation (SD) values include temporal variability across months in the yearly climatology and spatial variability across the global model domain. NPP = net primary production; DVM = diel vertical migration.

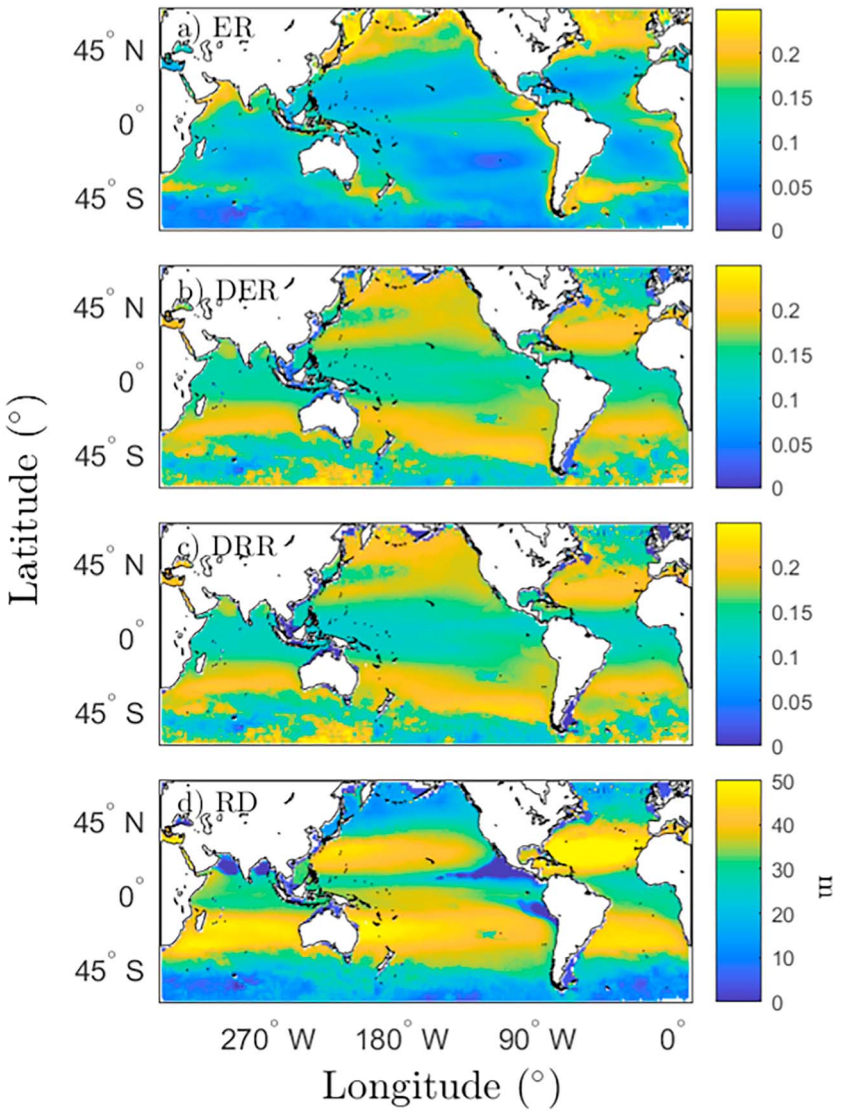

Figure 7. Global distribution of the (a) export ratio (ER), (b) DVM export ratio (DER), (c) DVM respiration ratio (DRR), and (d) respiration depression (RD). The value at each grid point is the annual mean over the seasonal cycle.

biomass but falls short of accurately describing the regional variability because it does not characterize anomalously high values of zooplankton biomass that have been observed. The spatial patterns in both the modeled zooplankton biomass and observations from COPEPOD show elevated values in regions of high NPP, most importantly in shelf waters around the globe. However, the COPEPOD data show very high concentrations of zooplankton north of 60°N, particularly in the Bering Sea (Moriarty & O'Brien, 2013). Unfortunately, the model does a poor job of representing plankton ecosystems north of 60°N due to a lack of satellite coverage over the seasonal cycle. The limited spatial range of the model may partially explain why the model does not do a good job of describing the high end of the distribution of zooplankton biomass.

Finally, we compared model estimates of the DVM-mediated export flux to empirical observations (Figure 9). The active respiratory flux of carbon as a result of zooplankton DVM has been quantified in a number of locations based on vertical migrant biomass and estimates of metabolic rates (Isla et al., 2015). Suitable data for comparison to the model exist for BATS (Steinberg et al., 2000), the equatorial Pacific (Zhang & Dam, 1997), ALOHA (Al-Mutairi & Landry, 2001), the North Atlantic (Isla & Anadon, 2004; Longhurst et al., 1990), the Canary Islands (Hernández-León et al., 2001), and the California Current (Stukel et al., 2013). Overall, the model does a good job of capturing broad patterns in the magnitude of the DVM-mediated export flux. To first order, the model predicts higher DVM export fluxes at the stations where the active respiratory

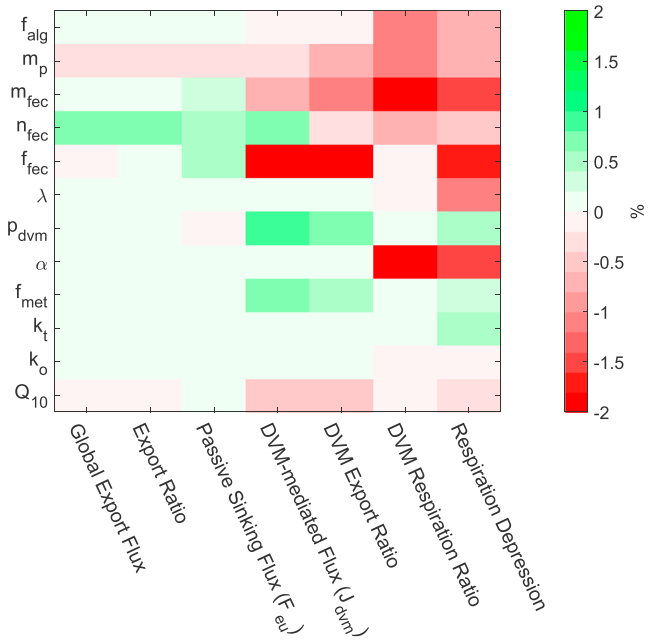

Figure 8. Results of the sensitivity analysis. Each box represents the percent change in the model output based on a 1% increase in the parameter value. Parameter rows with zero sensitivity on all the output metrics have been excluded. DVM = diel vertical migration.

flux has been observed to be larger. However, plotting the data does reveal the model is consistently overestimating the DVM export flux. There are a number of important parameters, which have a linear relationship with model outputs (Figure 8), which may be contributing to the discrepancy between the model and observations. While we made no attempt at optimization for this misfit, as it is outside the scope of this contribution, small changes to parameter values such as p_{dvm} would likely bring the model estimates more in line with observations. Only rarely have numerical models been used to quantify the DVM-mediated export fluxes on global scales. A recent study by Aumont et al. (2018) created a synthesis of the NEMO-PISCES and Apex Predators ECOSystem models tuned with empirical observations of zooplankton biomass to estimate DVM-mediated export.

Elevated contributions of DVM activity to export and mesopelagic biogeochemistry in the subtropical latitudes results from the combined effect of multiple contributing physical and biological factors. Reduced chlorophyll concentrations at the surface and high incident irradiance levels in subtropical latitudes means that the target isolume is deeper in the water column, resulting in increased migration depths. Additionally, higher values of $\mathrm{NPP}_n/\mathrm{NPP}_m$ results in smaller fluxes of sinking particles with respect to other sources of export, including active transport by DVM, since nanophytoplankton do not sink out of the euphotic zone. Increased temperature also modulates biogeochemical activity and plays a role in determining the effect of DVM. Higher temperature decreases the characteristic remineralization length scale and shoals the remineralization profile (Laufkötter et al., 2017; Marsay et al., 2015), making the localized input of DIC into the twilight zone by DVM a larger perturbation. In contrast, a steeper temperature vertical gradient reduces

Table 4
Summary of the Comparisons Between Model Output at BATS and In Situ Observations Made at the Bermuda Atlantic Time Series Scientific Station

Statistic	Model mean (SD)	Observation mean (SD)	Percent difference (%)
Zooplankton biomass ($\mathrm{mgC/m^2}$)	3.5 (0.68)	1.16 (0.19)	100.6
Total export flux ($\mathrm{mgC{\cdot}m^{-2}{\cdot}day^{-1}}$)	18.8 (5.2)	25.8 (3.8)	31.4
Export ratio	0.07 (0.03)	0.06 (0.01)	15.4

Note. Observation means and standard deviations (SD) are taken from reviews by Steinberg et al. (2001) and Madin et al. (2001). BATS = Bermuda Atlantic Time Series.

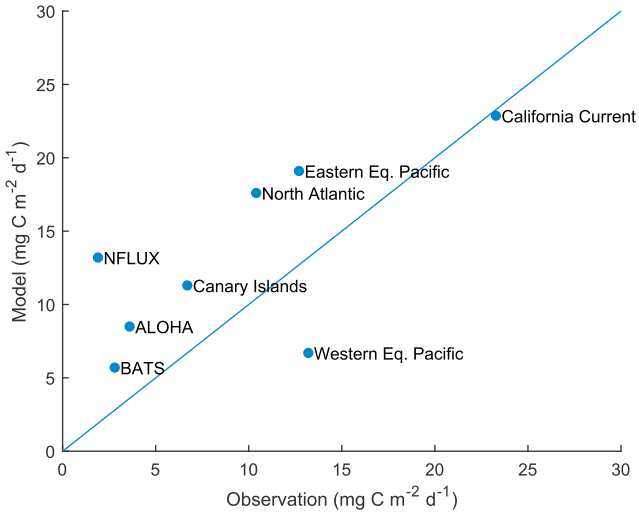

Figure 9. Comparison of model estimates of the diel vertical migration-mediated export flux to empirical observations at a variety of locations. A 1:1 line is included for reference. BATS = Bermuda Atlantic Time Series.

p_{met}, due to the increased temperature difference between the surface and the euphotic zone (equation (11)) and tends to make the fraction of absorbed carbon metabolized in the twilight zone (J_{met}) smaller. We can infer from the increased values of respiration depression in the subtropics (Figure 7) that the shoaling of the sinking POC remineralization profile has a greater effect than the reduction of J_{met}. A larger respiration depression indicates that carbon will generally be deposited deeper in the water column as a result of DVM activity, into water that is older and further removed from the atmosphere (Kwon et al., 2009).

Overall, the contribution of DVM activity to DIC production and oxygen utilization in the twilight zone was larger than its contribution to the vertical POC flux, indicating that the impacts of DVM are primarily respiratory in nature. One important result of increased DVM is an oxygen utilization profile that does not decrease monotonically with depth. While the remineralization of sinking particles does decrease monotonically over the water column, this is only one of the processes that contribute to total oxygen utilization in the twilight zone. Respiration rates by vertically migrating zooplankton account for a significant portion of the total oxygen utilization. In locations where DVM is an important contributor to water column DIC production, the presence of migrating zooplankton should produce a significant oxygen utilization spike at depth. The distribution over depth and the maximum magnitude of this spike depends on the parameterized width of the Gaussian used to distribute estimated zooplankton metabolism. We used observations of the thickness of migrating zooplankton layers to parameterize the model (Bianchi & Mislan, 2016) but did not allow for these parameters to change over the model domain. In real populations, regional differences in the representation by different taxa and intraspecific variations may result in a source of DIC production that is either more narrow or more diffuse than presented here. For smaller-scale applications of the model, instead of parameterizing the distribution of zooplankton around a mean depth, it should be possible to define the depth and thickness of the migrating zooplankton layer using acoustic data. Regardless, model results imply that respiration by migrating zooplankton makes up a significant proportion of total water column oxygen utilization and DVM should have important impacts on the magnitude and vertical structure of the oxygen utilization profile within the twilight zone.

The model makes a number of simplifying assumptions concerning remineralization and vertical migrations in the twilight zone. First, we have chosen to treat sinking POC as a single pool of carbon that is remineralized using an exponential decay model. Alternative parameterizations exist, however, which include additional information about variable remineralization rates, sinking speeds, and particle compositions. Two popular alternatives are the Martin Curve (Martin et al., 1987) and the Ballast Hypothesis (Armstrong et al., 2002). The Martin Curve model uses a normalized power function, which, compared to the exponential decay model used here, is equivalent to incorporating remineralization rates that decline with depth or sinking speeds that increase with depth. The Ballast Hypothesis model assumes that certain minerals associated with the POC flux (including silicate, calcium carbonate, and dust) serve to increase the total export flux by increasing sinking speeds and protecting POC from microbial remineralization. Despite the conceptual differences between these three models, an evaluation of the performance of the three models in different biogeochemical regimes by Gloege et al. (2017) found that the exponential model performs equally well to the Martin Curve and the Ballast Hypothesis models over most of the twilight zone. Below 1,000 m, the exponential decay model tended to underestimate the export flux because it does not account for variable remineralization length scales (Gloege et al., 2017). However, the depth scale of the model was set by the depth of DVM, which was shallow enough that considerations about sinking particles below 1 km were not relevant. The exponential decay model also has the advantage of increased simplicity with fewer parameters compared to alternative remineralization models, which is advantageous for the exploratory nature of this study.

Another important simplifying assumption of this model is the representation of DVM. In the ocean, many populations of zooplankton and fish participate in vertical migrations over many different and overlapping depth ranges and some of these populations do not ever enter the euphotic zone. This system of

interconnected vertical migrations that passes POC down into the twilight zone through depth-tiered populations has been described as Vinogradov's Ladder (Vinogradov, 1962) or the Bucket Brigade Hypothesis (Ochoa et al., 2013). The model described here integrates this system of vertical migrations into a single event that transports carbon from the euphotic zone to a target depth in the twilight zone, both for simplicity of illustration and due to a lack of data constraints. While the food web model of the euphotic zone provides constraints on grazing rates of zooplankton populations that spend at least some fraction of their time in the surface ocean, there is a lack of adequate data to fully parameterize the biological complexity of the bucket brigade hypothesis. The model instead represents an idealized scenario in which a single zooplankton migration is represented for the entire migrant community. The results presented here should be interpreted in the context of comparing model simulations which included DVM behavior to control runs which did not. As a result, interpretation of these results should be caveated by the acknowledgement that in real ecosystems, migration depth will vary significantly by taxa, including taxa whose diel migrations never go above the euphotic zone depth. As a result, the spike of DIC production and oxygen utilization seen in the model results is likely to be a more diffuse source spread out across the twilight zone.

The modeled global export flux is more robust to changes in the parameter values than the relative contribution of the passive sinking flux and the DVM-mediated flux to total export. This is not surprising, considering that the model represents multiple pathways that all sum to total export. However, the magnitude of the DVM-mediated export flux is highly sensitive to at least three parameters that have relatively high uncertainty in the model: f_{fec}, p_{dvm}, and f_{met}. In this study, we assumed that these parameters were constant across the global domain, but variations within and among zooplankton communities is expected to generate both spatial and temporal variability (Steinberg & Landry, 2017). For example, the proportion of zooplankton participating in DVM can vary anywhere from no DVM to a migration of nearly the entire community (Isla et al., 2015; Klevjer et al., 2016; Putzeys & Hernandez-Leon, 2005; Takahashi et al., 2009). This variability will exist both spatially between grid points and temporally over the seasonal cycle. The model also relies on very rough estimates of trophic efficiency to estimate the scaling factor of $n_{\mathrm{fec}} : m_{\mathrm{fec}}$ and variability in species composition and life history strategy will result in regional differences in this ratio. Additional work is needed to quantify the variability of these parameters in order to understand the effect of regional differences in zooplankton community characteristics on DVM-mediated carbon export. Translation between the parameters used in this model and traditional physiological measurements made by laboratory experiments is straightforward. For example, the assimilation efficiency of the large zooplankton size class is equation to $1 - m_{\mathrm{fec}}$ and the gross growth efficiency of micrograzers is equal to the ratio of $n_{\mathrm{fec}}/m_{\mathrm{fec}}$.

In addition to parameter uncertainty, the results may also be affected by structural uncertainty (e.g., additional trophic levels, mixotrophy). For example, additional trophic levels of zooplankton below the migrators would substantially diminish the impact of DVM due to further respiratory loss of grazed carbon at the surface. We have also designed the model such that none of the zooplankton mortality term contributes to the carbon export flux. The treatment of zooplankton mortality terms varies considerably in biogeochemical models, ranging from complete remineralization in the surface ocean to complete routing of the loss terms to the export flux (Laufkötter et al., 2016). We have assumed that biomass lost through zooplankton mortality is routed upward to higher trophic levels or remineralized in the euphotic zone but acknowledge that this assumption is likely to reduce our overall estimate of the global carbon export flux. In general, we have opted to use a simple food web model to investigate broad impacts of implementing DVM behaviors into an export model. We encourage future work that establishes how increasingly complex and realistic food web models influence the results presented here.

The model suggests that zooplankton respiration in the twilight zone is an important component of the export flux of the biological pump. As a result, empirical studies which quantify the export flux by measuring the sinking of POC throughout the water column (Eppley & Peterson, 1979; Henson et al., 2011) may be underestimating the export ratio. The pathway by which zooplankton graze phytoplankton biomass in the surface ocean and subsequently metabolize a portion of that biomass at depth is a significant component of the biological pump which completely circumvents the vertical POC flux. An accurate portrayal of the biological pump, both conceptually and quantitatively, should include the action of zooplankton DVM and its effect on both particle export and water column biogeochemistry (Buesseler & Boyd, 2009).

It has long been acknowledged that zooplankton vertical migrations play an important role in the biological pump and the biogeochemistry of the twilight zone. Respiratory models of the biological pump that

include DVM have estimated that the flux of carbon mediated by migrating zooplankton is 13% to 58% of the passive sinking flux (Longhurst et al., 1990) and accounts for up to 50% of the production of DIC in the twilight zone (Bianchi, Stock, et al., 2013). Results from our model are consistent with these observations and show significant contributions by zooplankton DVM to both carbon export and respiration in the twilight zone. However, despite solid evidence that DVM is a significant contributor to carbon export, the phenomenon is often excluded from global models of the biological pump, perhaps in part due to the difficulty in parameterizing the process. This study provides a valuable first step in quantifying the global variability in DVM-mediated contributions to the biological pump. Additionally, and equally important, it provides a relatively straightforward parameterization of zooplankton DVM that could be implemented in a global model as a basis for future investigations.

Acknowledgments
Support for this work came from the National Science Foundation (OCE-1434000 and OCE-1657803) and the National Aeronautics and Space Administration (NASA) as part of the EXport Processes in the global Ocean from RemoTe Sensing (EXPORTS) field campaign (grant 80NSSC17K0692) and the North Atlantic Aerosol and Marine Ecosystems Study (NAAMES, grants NNX15AE72G and 80NSSC18K0018). The satellite data used as drivers for the model are available as supporting information. The World Ocean Atlas data (World Ocean Atlas 2009, Annual Climatology, 1 degree, Temperature, Salinity, Oxygen) containing temperature and oxygen measurements can be downloaded from the ERDAPP data server (https://coastwatch.pfeg.noaa.gov/erddap/index.html).

References

Al-Mutairi, H., & Landry, M. R. (2001). Active export of carbon and nitrogen at Station ALOHA by diel migrant zooplankton. *Deep Sea Research Part II: Topical Studies in Oceanography*, *48*, 2083–2103. https://doi.org/10.1016/S0967-0645(00)00174-0

Armstrong, R. A., Lee, C., Hedges, J. I., Honjo, S., & Wakeham, S. G. (2002). A new, mechanistic model for organic carbon fluxes in the ocean based on the quantitative association of POC with ballast minerals. *Deep Sea Research Part II: Topical Studies in Oceanography*, *49*(1), 219–236. https://doi.org/10.1016/S0967-0645(01)00101-1

Atkinson, A., Ward, P., & Murphy, E. J. (1996). Diel periodicity of subantarctic copepods: Relationships between vertical migration, gut fullness and gut evacuation rate. *Journal of Plankton Research*, *18*(8), 1387–1405. https://doi.org/10.1093/plankt/18.8.1387

Aumont, O., Maury, O., Lefort, S., & Bopp, L. (2018). Evaluating the potential impacts of the diurnal vertical migration by marine organisms on marine biogeochemistry. *Global Biogeochemical Cycles*, *32*, 1622–1643. https://doi.org/10.1029/2018GB005886

Bautista, B., & Harris, R. P. (1992). Copepod gut contents, ingestion rates and grazing impact on phytoplankton in relation to size structure of zooplankton and phytoplankton during a spring bloom. *Marine Ecology Progress Series*, *82*(Cushing 1989), 41–50. https://doi.org/10.3354/meps082041

Bianchi, D., Galbraith, E. D., Carozza, D. A., Mislan, K. A. S., & Stock, C. A. (2013). Intensification of open-ocean oxygen depletion by vertically migrating animals. *Nature Geoscience*, *6*, 545–548. https://doi.org/10.1038/ngeo1837

Bianchi, D., & Mislan, K. A. (2016). Global patterns of diel vertical migration times and velocities from acoustic data. *Limnology and Oceanography*, *61*(1), 353–364. https://doi.org/10.1002/lno.10219

Bianchi, D., Stock, C., Galbraith, E. D., & Sarmiento, J. L. (2013). Diel vertical migration: Ecological controls and impacts on the biological pump in a one-dimensional ocean model. *Global Biogeochemical Cycles*, *27*, 478–491. https://doi.org/10.1002/gbc.20031

Boyd, P. W., Gall, M. P., Silver, M. W., Coale, S. L., Bidigare, R. R., & Bishop, J. K. B. (2008). Quantifying the surface-subsurface biogeochemical coupling during the VERTIGO ALOHA and K2 studies. *Deep Sea Research Part II: Topical Studies in Oceanography*, *55*(14-15), 1578–1593.

Buesseler, K. O., & Boyd, P. W. (2009). Shedding light on processes that control particle export and flux attenuation in the twilight zone of the open ocean. *Limnology and Oceanography*, *54*(4), 1210–1232. https://doi.org/10.4319/lo.2009.54.4.1210

Dam, H. G., & Peterson, W. T. (1988). The effect of temperature on the gut clearance rate constant of planktonic copepods. *Journal of Experimental Marine Biology and Ecology*, *123*(1), 1–14. https://doi.org/10.1016/0022-0981(88)90105-0

Doney, S. C., Glover, D. M., & Najjar, R. G. (1996). A new coupled, one-dimensional biological-physical model for the upper ocean: Applications to the JGOFS Bermuda Atlantic Time-series Study (BATS) site. *Deep Sea Research Part II: Topical Studies in Oceanography*, *43*(2-3), 591–624. https://doi.org/10.1016/0967-0645(95)00104-2

Eppley, R. W., & Peterson, B. J. (1979). Particulate organic matter flux and planktonic new production in the deep ocean. *Nature*, *282*(5740), 677–680.

Falkowski, P. G., Barber, R. T., & Smetacek, V. (1998). Biogeochemical controls and feedbacks on ocean primary production. *Science*, *281*(1998), 200–206. https://doi.org/10.1126/science.281.5374.200

Fasham, M. J. R., Ducklow, H. W., & McKelvie, S. M. (1990). A nitrogen-based model of plankton dynamics in the oceanic mixed layer. *Journal of Marine Research*, *48*(3), 591–639. https://doi.org/10.1357/002224090784984678

Fischer, J., & Visbeck, M. (1993). Seasonal variation of the daily zooplankton migration in the Greenland Sea. *Deep Sea Research Part I: Oceanographic Research Papers*, *40*(8), 1547–1557.

Forsythe, W. C., Rykiel, E. J., Stahl, R. S., Wu, H. i., & Schoolfield, R. M. (1995). A model comparison for daylength as a function of latitude and day of year. *Ecological Modelling*, *80*(1), 87–95. https://doi.org/10.1016/0304-3800(94)00034-F

Gloege, L., McKinley, G. A., Mouw, C. B., & Ciochetto, A. B. (2017). Global evaluation of particulate organic carbon flux parameterizations and implications for atmospheric pCO_2. *Global Biogeochemical Cycles*, *31*, 1192–1215. https://doi.org/10.1002/2016GB005535

Haney, J. F. (1988). Diel patterns of zooplankton behaviour. *Bulletin of Marine Science*, *43*(3), 583–603.

Hays, G. C. (2003). A review of the adaptive significance and ecosystem consequences of zooplankton diel vertical migrations. *Hydrobiologia*, *503*, 163–170. https://doi.org/10.1023/B:HYDR.0000008476.23617.b0

Henson, S. A., Sanders, R., Madsen, E., Morris, P. J., Le Moigne, F., & Quartly, G. D. (2011). A reduced estimate of the strength of the ocean's biological carbon pump. *Geophysical Research Letters*, *38*, L04606. https://doi.org/10.1029/2011GL046735

Hernández-León, S., Gómez, M., Pagazaurtundua, M., Portillo-Hahnefeld, A., Montero, I., & Almeida, C. (2001). Vertical distribution of zooplankton in Canary Island waters: Implications for export flux. *Deep Sea Research Part I: Oceanographic Research Papers*, *48*(4), 1071–1092. https://doi.org/10.1016/S0967-0637(00)00074-1

Ikeda, T. (2014). Respiration and ammonia excretion by marine metazooplankton taxa: Synthesis toward a global-bathymetric model. *Marine Biology*, *161*(12), 2753–2766. https://doi.org/10.1007/s00227-014-2540-5

Isla, A., & Anadon, R. (2004). Mesozooplankton size-fractionated metabolism and feeding off NW Spain during autumn: Effects of a poleward current. *ICES Journal of Marine Science*, *61*(4), 526–534. https://doi.org/10.1016/j.icesjms.2004.03.014

Isla, A., Scharek, R., & Latasa, M. (2015). Zooplankton diel vertical migration and contribution to deep active carbon flux in the NW Mediterranean. *Journal of Marine Systems*, *143*, 86–97. https://doi.org/10.1016/j.jmarsys.2014.10.017

Klevjer, T. A., Irigoien, X., Røstad, A., Fraile-Nuez, E., Benítez-Barrios, V. M., & Kaartvedt, S. (2016). Large scale patterns in vertical distribution and behaviour of mesopelagic scattering layers. *Scientific Reports*, *6*, 19873. https://doi.org/10.1038/srep19873

Kwon, E. Y., Primeau, F., & Sarmiento, J. L. (2009). The impact of remineralization depth on the air-sea carbon balance. *Nature Geoscience*, *2*(9), 630–635. https://doi.org/10.1038/ngeo612

Lampert, W. (1989). The adaptive significance of diel vertical migration of zooplankton. *Functional Ecology*, *3*(1), 21–27. https://doi.org/10.2307/2389671

Last, K. S., Hobbs, L., Berge, J., Brierley, A. S., & Cottier, F. (2016). Moonlight drives ocean-scale mass vertical migration of zooplankton during the Arctic winter. *Current Biology*, *26*(2), 244–251. https://doi.org/10.1016/j.cub.2015.11.038

Laufkötter, C., John, J. G., Stock, C. A., & Dunne, J. P. (2017). Temperature and oxygen dependence of the remineralization of organic matter. *Global Biogeochemical Cycles*, *31*, 1038–1050. https://doi.org/10.1002/2017GB005643

Laufkötter, C., Vogt, M., Gruber, N., Aumont, O., Bopp, L., Doney, S. C., et al. (2016). Projected decreases in future marine export production: The role of the carbon flux through the upper ocean ecosystem. *Biogeosciences*, *13*, 4023–4047. https://doi.org/10.5194/bg-13-4023-2016

Lima, I. D., Lam, P. J., & Doney, S. C. (2014). Dynamics of particulate organic carbon flux in a global ocean model. *Biogeosciences*, *11*(4), 1177–1198. https://doi.org/10.5194/bg-11-1177-2014

Longhurst, A. R., Bedo, A. W., Harrison, W. G., Head, E. J. H., & Sameoto, D. D. (1990). Vertical flux of respiratory carbon by oceanic diel migrant biota. *Deep Sea Research Part A, Oceanographic Research Papers*, *37*(4), 685–694. https://doi.org/10.1016/0198-0149(90)90098-G

Madin, L. P., Horgan, E. F., & Steinberg, D. K. (2001). Zooplankton at the Bermuda Atlantic Time-series Study (BATS) station: Diel, seasonal and interannual variation in biomass, 1994–1998. *Deep-Sea Research Part II: Topical Studies in Oceanography*, *48*(8-9), 2063–2082. https://doi.org/10.1016/S0967-0645(00)00171-5

Marsay, C. M., Sanders, R. J., Henson, S. A., Pabortsava, K., Achterberg, E. P., & Lampitt, R. S. (2015). Attenuation of sinking particulate organic carbon flux through the mesopelagic ocean. *Proceedings of the National Academy of Sciences*, *112*(4), 1089–1094. https://doi.org/10.1073/pnas.1415311112

Martin, J. H., Knauer, G. A., Karl, D. M., & Broenkow, W. W. (1987). VERTEX: Carbon cycling in the northeast Pacific. *Deep Sea Research Part A. Oceanographic Research Papers*, *34*(2), 267–285. https://doi.org/10.1016/0198-0149(87)90086-0

Michaels, A. F., & Silver, M. W. (1988). Primary production, sinking fluxes and the microbial food web. *Deep-Sea Research*, *35*(4), 473–490.

Moore, J. K., Doney, S. C., & Lindsay, K. (2004). Upper ocean ecosystem dynamics and iron cycling in a global three-dimensional model. *Global Biogeochemical Cycles*, *18*, GB4028. https://doi.org/10.1029/2004GB002220

Moriarty, R., & O'Brien, T. D. (2013). Distribution of mesozooplankton biomass in the global ocean. *Earth System Science Data*, *5*(1), 45–55. https://doi.org/10.5194/essd-5-45-2013

Ochoa, J., Maske, H., Sheinbaumc, J., & Candela, J. (2013). Diel and lunar cycles of vertical migration extending to below 1000 m in the ocean and the vertical connectivity of depth-tiered populations. *Limnology and Oceanography*, *58*(4), 1207–1214. https://doi.org/10.4319/lo.2013.58.4.1207

Putzeys, S., & Hernandez-Leon, S. (2005). A model of zooplankton diel vertical migration off the Canary Islands: Implication for active carbon flux. *Journal of Sea Research*, *53*(4), 213–222. https://doi.org/10.1016/j.seares.2004.12.001

Siegel, D. A., Buesseler, K. O., Behrenfeld, M. J., Benitez-Nelson, C. R., Boss, E., Brzezinski, M. A., et al. (2016). Prediction of the export and fate of global ocean net primary production: The EXPORTS science plan. *Frontiers in Marine Science*, *3*(March), 1–10. https://doi.org/10.3389/fmars.2016.00022

Siegel, D. A., Buesseler, K. O., Doney, S. C., Sailley, S., Behrenfeld, M. J., & Boyd, P. W. (2014). Global assessment of ocean carbon export by combining satellite observations and food-web models. *Global Biogeochemical Cycles*, *28*, 181–196. https://doi.org/10.1002/2013GB004743

Son, S., & Wang, M. (2015). Diffuse attenuation coefficient of the photosynthetically available radiation Kd(PAR) for global open ocean and coastal waters. *Remote Sensing of Environment*, *159*, 250–258. https://doi.org/10.1016/j.rse.2014.12.011

Steinberg, D. K., Carlson, C. A., Bates, N. R., Goldthwait, S. A., Madin, L. P., & Michaels, A. F. (2000). Zooplankton vertical migration and the active transport of dissolved organic and inorganic carbon in the Sargasso Sea. *Deep-Sea Research Part I: Oceanographic Research Papers*, *47*(1), 137–158. https://doi.org/10.1016/S0967-0637(99)00052-7

Steinberg, D. K., Carlson, C. A., Bates, N. R., Johnson, R. J., Michaels, A. F., & Knap, A. H. (2001). Overview of the US JGOFS Bermuda Atlantic Time-series Study (BATS): A decade-scale look at ocean biology and biogeochemistry. *Deep-Sea Research Part II: Topical Studies in Oceanography*, *48*(8-9), 1405–1447. https://doi.org/10.1016/S0967-0645(00)00148-X

Steinberg, D. K., Goldthwait, S. A., & Hansell, D. A. (2002). Zooplankton vertical migration and the active transport of dissolved organic and inorganic nitrogen in the Sargasso Sea. *Deep-Sea Research Part I*, *49*(8), 1–17. https://doi.org/10.1016/S0967-0637(02)00037-7

Steinberg, D. K., & Landry, M. R. (2017). Zooplankton and the ocean carbon cycle. *Annual Review of Marine Science*, *9*(1), 413–444. https://doi.org/10.1146/annurev-marine-010814-015924

Stukel, M., Ohman, M., Benitez-Nelson, C., & Landry, M. (2013). Contributions of mesozooplankton to vertical carbon export in a coastal upwelling system. *Marine Ecology Progress Series*, *491*, 47–65. https://doi.org/10.3354/meps10453

Takahashi, K., Kuwata, A., Sugisaki, H., Uchikawa, K., & Saito, H. (2009). Downward carbon transport by diel vertical migration of the copepods Metridia pacifica and Metridia okhotensis in the Oyashio region of the western subarctic Pacific Ocean. *Deep-Sea Research Part I: Oceanographic Research Papers*, *56*(10), 1777–1791. https://doi.org/10.1016/j.dsr.2009.05.006

Vinogradov, M. (1962). Feeding of the deep-sea zooplankton. *Rapp Rv Réun Cons Perm Int Explor Mer*, *153*, 114–119.

Wallace, M. I., Cottier, F. R., Brierley, A. S., & Tarling, G. A. (2013). Modelling the influence of copepod behaviour on faecal pellet export at high latitudes. *Polar Biology*, *36*(4), 579–592. https://doi.org/10.1007/s00300-013-1287-7

Zhang, X., & Dam, H. G. (1997). Downward export of carbon by diel migrant mesozooplankton in the central equatorial Pacific. *Deep Sea Research Part II: Topical Studies in Oceanography*, *44*(9-10), 2191–2202. https://doi.org/10.1016/S0967-0645(97)00060-X